Numerical Simulation of Bridge Damage under Blast Loads

RONG-BING DENG [a], XIAN-LONG JIN [a,b]
a. High Performance Computing Center, School of Mechanical Engineering
b. State Key Laboratory of Mechanical system & Vibration
Shanghai Jiao Tong University
Room 225, Building B, School of Mechanical Engineering, No. 800 Dongchuan Road, Shanghai 200240
CHINA
rbdeng@sjtu.edu.cn http://webmail1.sjtu.edu.cn/

Abstract: - The numerical simulation of the structural damage of a steel truss bridge subjected to blast loading with the aid of a hydrocode is presented in this paper. A three-dimensional nonlinear finite element model of an actual bridge has been developed based on the drawing design of the Minpu II Bridge in Shanghai. The effects of mesh size on pressure distribution produced by explosions are also studied. Through the comparison between the calculation results and the experimental values, the reliability of the calculation is validated. All the process from the detonation of the explosive charge to deck crack, including the propagation of the blast wave and its interaction with the structure is reproduced. The numerical results show the damage of bridge parts and provide a global understanding of bridge under blast loads. It may be generated to supplement experimental studies for developing appropriate blast-resistant design guidelines for bridges in the future.

Key-Words: - steel truss bridge, blast load, hydrocode, bridge damage, ALE method, numerical simulation

1 Introduction

Bridges are crucial to a nation's transportation infrastructure. Due to different terrorist attacks all around the world, increased attention has been given to bridges which are vulnerable to blast loads. Bridge engineers, however, have not typically considered security in the design process. There are definite rules for resistance of wind, earthquake and ship collision, but no preventive measure for blast is addressed. Blast resistant analysis of bridges is a new and challenging project [1-4]. Therefore, it is of important military value and realistic meaning to simulate and study the damage effect of bridge under blast loads in order to provide useful reference for safety protection in the future.

Generally speaking, blast in air is characterized as short duration dynamic loading which significantly influences structural response. The frequencies of explosive loads can be much higher than conventional loads. Furthermore, short duration dynamic loads often exhibit strong spatial and time variations, resulting in sharp stress gradients in the structures. Consequently, the analysis of bridge structures subjected to blast loading becomes a very complex issue and it is hard to analyze accurately deformation or crack conditions of bridges subjected to blast wave using equations. On the other hand, experiments on real bridge are so exhibitive that it is hardly carried out. Historically, the analysis of explosions either has predominantly involved simplified analytical methods [5-7] or has required the use of supercomputers for detailed numerical simulations due to the fact that simulation of explosion is highly complicated, involving an explosion causing a shock wave propagation in air and then interaction with a structure. In recent years, many efforts have been devoted to the development of reliable methods and algorithms for a more realistic analysis of structures and structural components subjected to blast loading. Furthermore, with the rapid development of computer hardware over the last decades, it has become possible to make detailed numerical simulations of explosive events in personal computers. Moreover, new developments in integrated computer hydrocodes complete the tools necessary to carry out the numerical analysis successfully.

Hydrocodes are computational mechanics tools that simulate the response of both solid and fluid material under highly dynamic conditions (e.g., detonation and impact) where shock wave propagation is a dominant feature. Hydrocodes make fewer approximations than either of the more special-purpose Computational Fluid Dynamics (CFD) or Computational Solid Mechanics (CSM) methods. They numerically solve the more

fundamental time-dependent equations of continuum mechanics that CFD and CSM do not. Hydrocodes are tools for simulation of multi-material, compressible, transient continuum mechanics [8].

This paper is related to the effect of blast loads in bridges and presents the results of the numerical simulation of the damage of an actual bridge, the Minpu II bridge in Shanghai. It is assumed that the damage was caused by an explosive load equivalent to 800 kg of TNT placed on top of bridge deck. In this paper, the hydrocode ANSYS AUTODYN [9] is used for these purposes. The program is an integrated analysis program specifically designed for non-linear dynamics problems that uses finite difference, finite volume, and finite element techniques to solve a wide variety of non-linear problems in solid, fluid and gas dynamics. It has been used extensively in the defense industry for modelling blast-structure interaction. The phenomena to be studied with such a code can be characterized as highly time dependent with both geometric non-linearities (e.g. large strains and deformations) and material non-linearities (e.g. plasticity, failure, strain-hardening and softening, multiphase equations of state). The hydrocode uses a coupled methodology to allow an optimum numerical solution for a given problem. With this approach, different domains of a physical problem, e.g. structures, fluids, gases, etc. can be modelled with different numerical techniques or processors most appropriate for that domain. Then these different domains are coupled together in space and time to provide an optimized solution. This capability makes this code especially suitable for the study of interaction problems involving multiple systems of structures, fluids, and gases. Therefore, the dydrocode is widely applied to the modelling and analysis of impact, penetration, blast and explosion events [10-12].

In order to reproduce the structural damage, the complete bridge is modelled, including steel girder, cables, H-shaped bridge tower, piers and pier caps. Appropriate numerical models are used for the different materials in the bridge. In addition, the volume of air in which the bridge is immersed is also modelled. The analysis begins with the modelling of the detonation and propagation of the pressure wave inside the explosive and in the air in contact with the explosive. As this analysis must be performed with much detail, a spherical explosive is modelled. The distributions of pressures in different mesh sizes are compared with experimental values and a proper mesh size used for the analysis is chosen validating the simulation procedure. Then the results of this first analysis are mapped into the 3D model. Starting from this point, the propagation of the blast wave in air and its interaction with the building is simulated. In this way, the complete damage process is reproduced and analyzed. The paper is organized as follows. Section 2 presents the explicit time integration and Arbitrary Lagrangian-Eulerian (ALE) Method. Section 3 describes the numerical model for blast-bridge problem. Section 4 gives some simulation and experiment results. Section 5 provides some conclusions.

2 Methodology

All numerical techniques require the complex problem to be broken up into a finite number of smaller, simpler problems. This is a discretisation process. The equations need to be discretised both in time and space. The temporal discretisation is the same for different analysis techniques (processor) in AUTODYN. The complete time span is split into thousands of small time steps. Explicit time integration is used for computing required variables for process analysis. But the spatial discretisation is different for different processors. Three different schemes are included, Lagrange, Eulerian and Arbitrary Lagrangian-Eulerian (ALE). In this analysis, ALE method is applied to the blast-bridge problem.

2.1 Explicit Time Integration

Under blast loads, the dynamic equation of the bridge structure system can be defined as:

$$M\ddot{q} + C\dot{q} + f_{\text{int}} = f_{ext} \quad (1)$$

$$f_{\text{int}} = Kq(t) \quad (2)$$

where $q(t)$, $\dot{q}(t)$, $\ddot{q}(t)$ are the vectors of generalized displacements, velocities and accelerations, M , K and C are the mass, stiffness and damping matrices respectively, f_{int} is the vector of the internal resisting forces and f_{ext} is the vector of the external applied forces. The internal forces include the shares of material and geometric nonlinearities. Therefore the internal force vector has to be updated at each time step as well as each iteration step during the time integration of the equations of motion.

Contrary to implicit schemes the generation and factorization of system matrices, which are very memory and time consuming, may be avoided by explicit schemes (lumped mass and damping matrices). Working with system vectors (instead of

system matrices), which may be added up by the finite element contributions, for the computation of the state variables q and $\dot{q}$, it is possible to increase the number of degrees of freedom and thus large engineering problems can be treated. From software development point of view the application of the explicit time integration schemes provides the opportunity to create a uniform software concept both for the solution of static and dynamic problems. The central difference method to approximate q and $\dot{q}$ has proved to be a very effective procedure to integrate the initial value problem (1).

$$\dot{q}^t = \frac{1}{\Delta t}\left(q^{t+(1/2)\Delta t} - q^{t-(1/2)\Delta t}\right)$$
$$\ddot{q}^t = \frac{1}{\Delta t}\left(\dot{q}^{t+(1/2)\Delta t} - \dot{q}^{t-(1/2)\Delta t}\right) \quad (3)$$

Unfortunately, explicit methods are only conditionally stable and so the time step size has to be smaller than a critical value, which is directly dependent on the largest frequency of the finite element discretization (smallest element). The stability consideration of the central difference scheme gives a limitation of the time step length of

$$\Delta t_{krit} \le \frac{2}{\omega_{\max}} \quad (4)$$

where $\omega_{\max}$ is the highest frequency of the FE model. If we insert the Eq. (3) in Eq. (1), accept $C = cM$ with a lumped mass matrix M, the explicit solution scheme of Eq. (1) may be written as

$$\dot{q}_i^{t+(1/2)\Delta t} = \frac{2 - c^t \Delta t}{2 + c^t \Delta t}\dot{q}^{t-(1/2)\Delta t} + \frac{2\Delta t}{m_{ii}(2 + c^t \Delta t)}\left(f_{ext_i}^t - f_{int_i}^t\right)$$
$$q_i^{t+\Delta t} = q_i^t + \Delta t \dot{q}_i^{t+(1/2)\Delta t} \quad (5)$$

In Eq. (5) $f_{int_i}^t$ is the internal force related to the degree of freedom i, and $f_{ext_i}^t$ is the given external force at the degree of freedom i. The largest eigenvalue of a matrix is always smaller than any matrix norm (known as Gerschgorin's theorem), and from this follows the estimation:

$$\omega_i^2 \le \frac{1}{m_{ii}} \sum_{j=1}^{n} \left|k_{ij}\right| \quad (6)$$

where m_{ii} is the diagonal element of the lumped mass matrix. Substitution of Eq. (4) in Eq. (6) gives an estimation of m_{ii}:

$$m_{ii} \ge \frac{1}{4}\Delta t^2 \sum_{j=1}^{n} \left|k_{ij}\right| \quad (7)$$

The damping coefficient c included in (5) may be calculated from the condition of an aperiodic oscillation, i.e.

$$\upsilon = 1 = \frac{c}{2\omega_0} \quad (8)$$

where υ, c, ω_0 are the decrement of the damping, the damping coefficient and the smallest eigenfrequency, respectively. The smallest eigenfrequency ω_0 is approximated by the Rayleigh's quotient of the FE system, i.e.

$$\omega_0^2 \le \frac{q^{t^T} K q^t}{q^{t^T} M q^t} \quad (9)$$

The substitution of Eq. (9) in Eq. (10) gives the damping factor as

$$c^t = 2\sqrt{\frac{q^{t^T} K q^t}{q^{t^T} M q^t}} \quad (10)$$

It should be noted that the quadratic forms in Eqs. (9) and (10) are simply calculated at the element level by adding up the shares of each element.

2.2 Arbitrary Lagrangian-Eulerian Finite Element Method

The ALE method combines the advantages of purely Lagrangian method and purely Eulerian method.

Purely Lagrangian methods are typically used only for structural deformation. The mesh moves in space whereas the computational mesh of a Lagrangian model remains fixed on the material. Since the mass in each element remains fixed, no mass flux at inter-element boundaries must be computed. Material distortions correspond to Lagrangian mesh distortions. Large distortions may result in reductions in time-steps and/or stoppage of the calculation and the mesh will need to be repaired manually in order to continue the calculation. This process is necessary every time the mesh becomes too distorted for the calculations to continue. Therefore, the general limitation of most Lagrangian hydrocodes to relatively low-distortion computations limits their applicability to shock-structure interaction analysis and the explosion event is not feasible using a purely Lagrangian method due to the high deformation of the fluid mesh caused by the shockwave.

Purely Eulerian methods are typically used for fluid calculations. Eulerian hydrocodes advance solutions in time on a mesh fixed in space allowing the material passes through it, thus avoiding the Lagrangian mesh distortions problems. Eulerian

hydrocodes include material strength (flow of solids) and multi-material capabilities. Eulerian hydrocodes are strictly transient dynamics solvers. They are not designed to solve steady-state fluid flow problems. Eulerian hydrocodes are computationally expensive due to their ability to have elements that contain more than one material (i.e., multi-material elements). Numerical algorithms are required that prevent artificial material diffusion (the mixing of materials across a material interface) in mixed elements. The convergence to a common state parameter (e.g., pressure) in a multi-material element can also result in considerable expense. The Eulerian method does not cause mesh distortion, but it is not suitable for the analysis of structural deformation in blast-structure interaction.

Arbitrary Lagrangian Eulerian (ALE) hydrocodes share aspects with both Lagrangian and Eulerian hydrocodes; Lagrangian motion is computed every time step, followed by a remap phase in which the spatial mesh is either rezoned (Lagrangian), rezoned to its original shape (Eulerian) or rezoned to some "advantages" shape (between Lagrangian and Eulerian). ALE mesh motions are based primarily on the preservation of a uniform mesh, not the capture of physical phenomena. In other words, the approach is based on the arbitrary movement of a reference domain which, additionally to the common material domain and spatial domain, is introduced as a third domain. In this reference domain, which will later on correspond to the finite element mesh, the problem is formulated and the mesh is allowed to move, but the motion of the mesh does not necessarily coincide with the motion of the material. Therefore, it is easy to trace the free surfaces and moving boundaries accurately and to conserve the regularity of the computational mesh at the same time, coupling the fluid dynamics with the structural dynamics directly, without interfacing two separate coordinate systems. Structural elements can be incorporated directly in the ALE framework. The Arbitrary Lagrangian Eulerian method is the preferred method for assessing structural response due to an explosion in air for large deformations. The method provides the capabilities to model the fluid dynamics and the structural dynamics most efficiently by providing the accuracy of Lagrangian mesh motion and the robustness of Eulerian mesh motion within the same framework.

In the ALE description, the material derivative with respect to the reference coordinate can be described as follows: the ALE equations are derived by substituting the material time derivative with the reference configuration time derivative,

$$\frac{\partial f(X_i,t)}{\partial t} = \frac{\partial f(x_i,t)}{\partial t} + (\upsilon_i - u_i)\frac{\partial f(x_i,t)}{\partial x_i} = \frac{\partial f(x_i,t)}{\partial t} + \omega_i \frac{\partial f(x_i,t)}{\partial x_i} \quad (11)$$

where X_i is the Lagrangian coordinate, i is the referential coordinate, x_i is the Eulerian coordinate, ω_i is the reference velocities, and υ_i and u_i are the material and the mesh velocity components, respectively. Thus, the governing equations, including the equations of mass, momentum and energy conservation in a general ALE formulation are given by:

$$\frac{\partial \rho}{\partial t} = -\rho \frac{\partial \upsilon_i}{\partial x_i} - \omega_i \frac{\partial \rho}{\partial x_i} \quad (12)$$

$$\rho \frac{\partial \upsilon_i}{\partial t} = \sigma_{ij,j} + \rho b_i - \rho \omega_i \frac{\partial \upsilon_i}{\partial x_j} \quad (13)$$

$$\rho \frac{\partial E}{\partial t} = \sigma_{ij}\upsilon_{i,j} + \rho b_i \upsilon_i - \rho \omega_j \frac{\partial E}{\partial x_j} \quad (14)$$

where ρ is density, σ_{ij} is the components of the stress tensor, b_i is the body force, and E is the total energy.

The equations (12)-(14) are solved in two phases during each computational time step:

- The first step is the Lagrangian phase, during which the incremental motion of the material is computed and the material motion and the mesh motion are identical. Thus at the end of this cycle the position of the material surface is known.
- The second step is the Eulerian phase, which is referred to as the advection, or remap phase. In this step there is a transport of material between the cells because the mesh is moved independently to the material position. To keep a regular mesh the new remapping algorithm moves back the frontier nodes along the material surface determined in the Lagrangian cycle. Thus the position of the material surface is kept.

3 Numerical Model

3.1 Bridge Model

Figure 1 shows the schematic representation of the Minpu II bridge. The full-scale three dimensional finite-element model of the steel truss bridge is constructed following the actual design drawings. The resulting model is presented in Fig. 2. As it can

be seen in this figure, the bridge is composed of six differentiable parts: steel girder, cables, H-shaped bridge tower, transitional pier, auxiliary pier and pier cap. Except for the bridge stay cables, in which the individual cable strands are modelled by beam elements, all other major structural components are modelled with shell and solid elements. The complete model consists of 211949 nodes and 242186 elements. The whole bridge is solved with a Lagrange processor. The bottoms of the piers are fixed in their base corresponding to the ground level in the bridge.

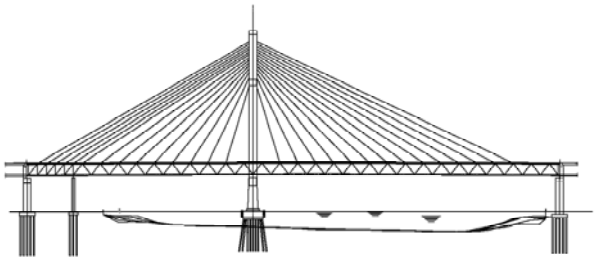

Fig.1 Schematic representation of bridge

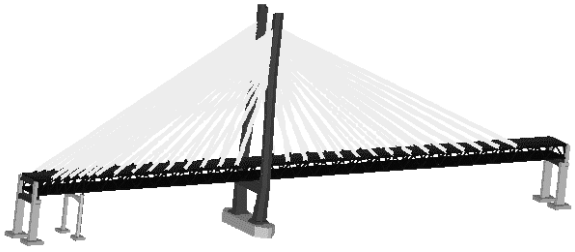

Fig.2 Three-dimensional finite element model of bridge

3.2 Generation of Blast Loading

It is quite a complex and tough task to study the dynamic responses of bridge components subjected to an explosive because the initiation of blast and the interaction between bridge and blast wave are included. In addition, computational resources are cost to the calculation of fluid cells. In order to reduce computational time and ensure the accuracy of results, the generation of blast loading in free air is based on remapping technology of ANSYS AUTODYN, which is a good method to calculate the initiation of detonation and the blast wave propagation in free air. So numerical analysis of the bridge under blast loads is performed in two stages. The first part of the analysis is the simulation of the explosion itself from the detonation instant and the propagation of the blast wave in air. The problem has spherical symmetry and can be treated as 1D. When solution time is reached, the remapping file is generated based on the model. The second part is the input of previous remapping file and analysis of the impact effect and interaction with the bridge of the blast wave. In this way, the results of 1D analysis are later mapped in the 3D model representing the bridge and the surrounded air volume drastically reducing the computational cost of numerical analysis.

In the first part of explosion generation, the use of symmetry conditions allows the spherical portion of the blast wave expansion to be represented by a spherical model. This is achieved by a one-dimensional (1D) mesh using spherical symmetry. The number of cells required to produce accurate solutions is greatly reduced when compared with a full 3D model. When the spherical blast wave begins to interact with obstacles, the flow becomes multi-dimensional. However, before this time, the 1D solution can be imposed or remapped onto a specific region of the multi-dimensional model. The 3D calculation can then proceed from that point.

In order to carry out a comparable analysis, the mass of the explosive is defined by TNT masses [7]. The corresponding masses for other explosives can be obtained through the concept of TNT equivalence [13]. In the analysis, the initial detonation and expansion of the sphere of 800 kg of TNT is modelled in a 1D, spherically symmetric model of 1.2m radius with a JWL equation of state, as illustrated in Fig. 3. The remapping of the 1D analysis to the 3D model of the bridge is shown in Fig. 4.

Fig.3 Mesh used for the generation of the explosion

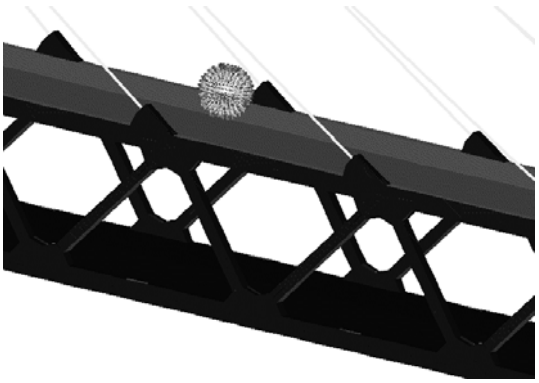

Fig.4 The location of blast on top of bridge （local view）

3.3. Material Constitutive Models

In order to develop a robust nonlinear finite element model of the steel truss bridge in computer simulation, it is important to select the proper material constitutive formulation for structural components.

The differential equations governing unsteady material dynamic motion are used to express the local conservation of mass, momentum and energy. In order to obtain a complete solution, it is necessary to define a further relation between the flow variables in addition to appropriate initial and boundary conditions. This can be found from a material model which relates stress to deformation and internal energy (or temperature). In most cases, the stress tensor may be separated into a uniform hydrostatic pressure (all three normal stresses equal) and a stress deviatoric tensor associated with the resistance of the material to shear distortion. Then the relation between the hydrostatic pressure, the local density (or specific volume) and local specific energy (or temperature) is known as an equation of state.

In this study, each component of the bridge structure has been given an appropriate material constitutive model. The principal mechanical properties of different material are presented in Table 1.

Table 1 Material properties used in computational model

Material	Equation of state	Strength model	Reference density ($g \cdot cm^{-3}$)	Shear Modulus (KPa)
TNT	JWL	None	1.63	None
Air	Ideal Gas	None	1.225E-3	None
Steel	Linear	Johnson Cook	7.85	7.923E+7
Reinforced concrete	P alpha	RHT Concrete	2.6	1.312E+7

4 Numerical Results

4.1 Blast analysis and verification

In order to study dynamic responses of structures subjected to blast loading, it is important to build computational model of blast first and describe blast generation, development and propagation in air correctly. The impact of blast wave to surrounding objects is mainly pressure effect, so the key of numerical simulation is calculation of peak overpressures.

The observed characteristics of air blast waves are found to be affected by the physical properties of the explosion source. Figure 5 shows a typical blast pressure profile. The detonation of a condensed high explosive generates hot gases and the hot gas expands forcing out the volume it occupies. As a consequence, a layer of compressed air (blast wave) forms in front of this gas volume containing most of the energy released by the explosion. At the arrival time t_a, following the explosion, pressure at that position suddenly increases to a peak value of overpressure, p_s, over the ambient pressure, p_0. After a short time, the pressure behind the front may drop below the ambient pressure. During such a negative phase, a partial vacuum is created and air is sucked in. This is also accompanied by high suction winds that carry the debris for long distances away from the explosion source.

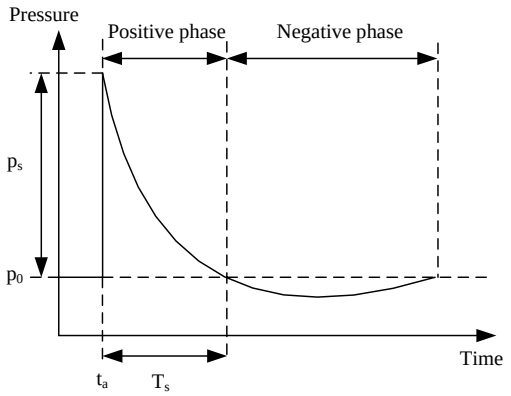

Fig.5 A typical pressure history for a blast wave

All blast parameters are primarily dependent on the amount of energy released by a detonation in the form of a blast wave and the distance from the explosion. A universal normalized description of the blast effects can be given by scaling distance relative to $(E/p_0)^{1/3}$ and scaling pressure relative to p_0, where E is the energy release (kJ) and p_0 the ambient pressure. For convenience, however, it is general practice to express the basic explosive input or charge weight W as an equivalent mass of TNT. Results are then given as a function of the dimensional distance parameter (scaled distance) $Z = R/W^{1/3}$, where R is the actual effective distance from the explosion. W is generally expressed in kilograms. Scaling laws provide

parametric correlations between a particular explosion and a standard charge of the same substance.

The pressure – time history of a blast wave is often described by exponential functions such as Friedlander equation [14] which has the form

$$p(t) = p_0 + p_s\left[1-(t-t_a)/T_s\right]\exp\left[-A(t-t_a)/T_s\right] \quad (15)$$

where t is the time, p_0 is the ambient pressure, p_s is the peak overpressure, T_s is the duration of the positive phase, t_a is the arrival time and A is a decay coefficient.

There are many solutions for the peak overpressures from both numerical solution and experimental measurements [5-7]. The results are usually presented in graphics, tables or equations based on experimental or numerical results, such as such as the representative Henrych equations presented by Smith and Hetherington [7].

The Henrych equations divide the analysis into three fields, a near, middle and far field. They are presented below.

$$p_s = \begin{cases} 1407.2/Z + 554.0/Z^2 \\ -35.7/Z^3 + 0.625/Z^4 KP_a \end{cases} \quad 0.05 \le Z \le 0.3$$

$$\begin{cases} 619.4/Z - 32.6/Z^2 \\ +213.2/Z^3 KP_a \end{cases} \quad 0.3 \le Z \le 1.0 \quad (16)$$

$$\begin{cases} 66.2/Z + 405.0/Z^2 \\ +328.8/Z^3 KP_a \end{cases} \quad 1.0 \le Z \le 10$$

Where p_s is the peak overpressure, $Z = R/W^{1/3}$, W is the charge mass expressed in kilograms of TNT, R is the distance from an explosive charge.

High explosives are chemical substances which, when subject to suitable stimuli, react chemically very rapidly releasing energy. In the hydrodynamic theory of detonation, this very rapid time interval is shrunk to zero and a detonation wave is assumed to be a discontinuity which propagates through the unreacted material instantaneously liberating energy and transforming the explosive into detonating products. The most comprehensive form of equation of state developed over this period, the "Jones–Wilkins–Lee" (JWL) equation of state is used in this paper,

$$p = C_1\left(1-\frac{\omega}{r_1 v}e^{-r_1 v}\right) + C_2\left(1-\frac{\omega}{r_2 v}e^{-r_2 v}\right) + \frac{\omega e}{v} \quad (17)$$

where p is the hydrostatic pressure, C_1, C_2, r_1 and r_2 are constants and e, ω and v are the internal energy, adiabatic constant and specific volume respectively.

It can be shown that at large expansion ratios the first and second terms on the right hand side of Eq. (17) become negligible and hence the behavior of the explosive tends towards that of an ideal gas. Therefore, at large expansion ratios, where the explosive has expanded by a factor of approximately 10 from its original volume, it is valid to switch the equation of state for a high explosive from JWL to ideal gas. In such a case the adiabatic exponent for the ideal gas, γ, is related to the adiabatic constant of the explosive, ω, by the relation $\gamma = \omega + 1$. The reference density for the explosive can then be modified and the material compression will be reset. Potential numerical difficulties are therefore avoided.

The accuracy of numerical results is strongly dependent on the mesh size used for the analysis. The coarser the mesh, the lesser accurate the computational is, and vice versa. Therefore, it is important to use an adequate mesh size in the numerical simulation of blast wave propagation in a long-span bridge. On the other hand, the mesh size is also limited by the dimensions of the model and the computer capacity. If the fluid mesh is too smaller, it will spend a lot of computational time and require more advanced computers. In order to save computational time and ensure computational accuracy, finer mesh is used in the interface of fluid and solid and coarser mesh in other regions.

In order to study the free propagation of blast waves in air, the air is numerically modelled with four different mesh sizes: 40, 50, 80 and 100 mm. A three dimensional Euler FCT (higher order Euler processor) subgrid is used for the air. The Euler-FCT processor has been optimized for gas dynamic problems and blast problems and it is much more efficient in comparison with a general purpose high resolution Euler processor. FCT stands for Flux Corrected Transport [15]. With FCT a high order solution is computed wherever this is possible in the flow field. The high order solution fluxes are corrected in the regions of shocks using a low order reference (transported and diffused) solution.

Figure 6 shows the comparison of numerical results for the peak overpressure with those obtained using empirical equations for different distances from the explosive charge. It can be seen that in the near field of detonation as the mesh is refined, the shorter distance between detonation point and object, the higher value peak overpressure is with peak

overpressure better agree with empirical equations. For large distances the effect of mesh size is relatively small. The accuracy of predictions and measurements in the near field is lower than in the far field, probably due to the complexity of blast phenomena [7]. The results corresponding to the meshes of 4 and 5 cm are almost coincident. It can be concluded that the mesh of 5cm gives an accurate solution to the problem.

Figure 7 shows a pressure–time history curve obtained from different distances. It can be seen that the pressures increased abruptly followed by a quasi-exponential delay back to ambient pressure and when the distance between blast and gauge increases, the pressure decreases. Such tendency is in good agreement with the propagation law of blast wave in air verifying the correction of numerical simulation.

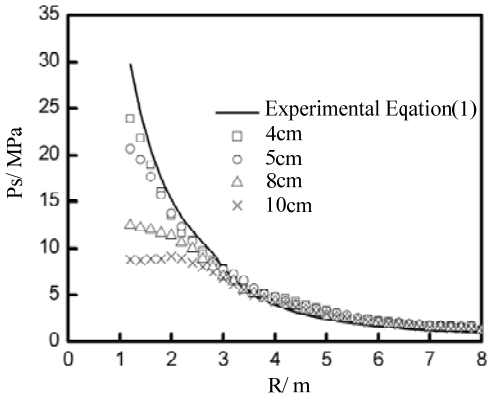

Fig.6 Variation of peak overpressures with distance

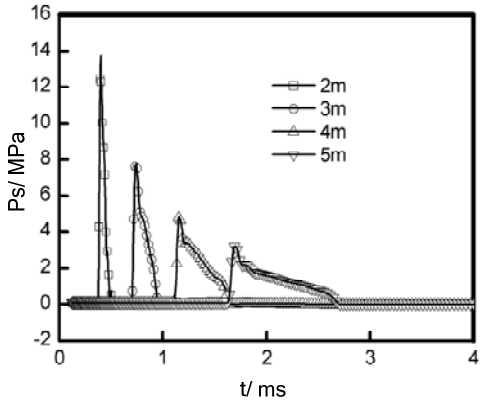

Fig.7 Variation of blast pressure with time

4.2 Interaction of Blast Wave with Bridge

To study the structural damage of the bridge, the propagation of the blast wave and its interaction with the bridge is analyzed. For that purpose, an interaction algorithm between the Lagrange (bridge) and Euler (air) processors is used.

As illustration of the role played by the interaction of the blast wave with the bridge, the propagation of the blast wave characterized by the velocity field of air in the actual bridge is shown in Fig. 8. It may be noted the alteration of the blast wave produced as a result of the multiple reflections on the steel truss. Because of the reflections on the deck, the blast wave lost its spherical shape and increased its destructive effect in vertical direction.

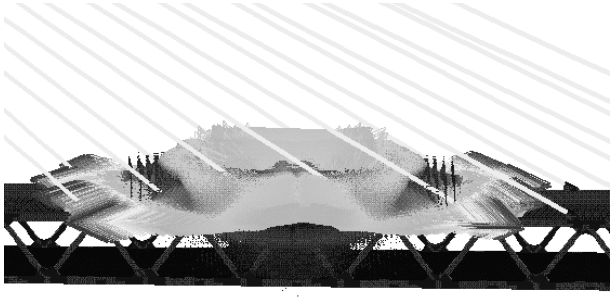

Fig. 8. Effect of the bridge in the blast wave propagation

4.3 Bridge Response

Figure 9 shows the stress distribution on bridge. The impact of blast wave to the whole bridge is observed through the stress distribution on whole bridge when the computational time 6ms is reached as presented in Fig. 9 (a). It can be seen that the parts surrounding the detonation undergo the rapid increase of stress whereas others far from the blast with much less value of stress even to zero. The stress concentrates in the limited region around the blast and plastic areas distribute in small areas of crack. It illustrates that the characteristic of damage effect of a blast load to the whole bridge is limited destruction zone near the blast, which corresponds to the general law of explosion [16].

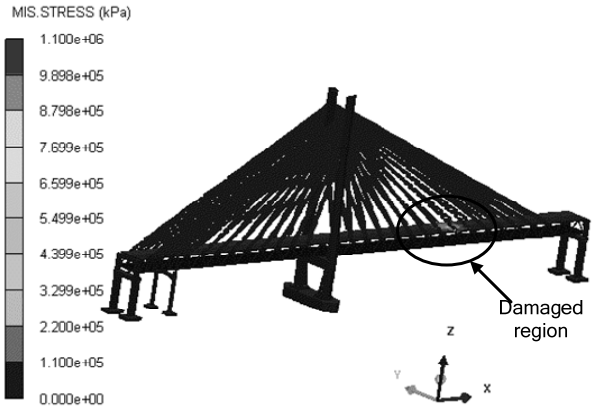

(a) whole bridge

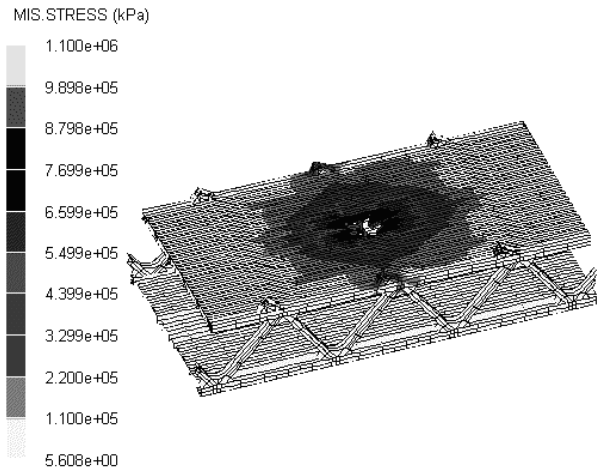

(b) local view

Fig.9 The stress distribution in bridge

The enlarged local stress distribution on bridge is shown in Fig.9 (b). For the sake of visualization, the cables are removed from the bridge model. In the analysis of the bridge damage, the solid–solid interaction between the different parts of the bridge damaged is also taken into account. It is clear that the parts face the explosion suffer the crushing or the disintegration of the material under intensive pressure waves. In order to reproduce this type of effects, the erosion model was used to remove from the calculus the cells that have reached certain criteria based on deformations. When a cell is eliminated, its mass is retained and concentrated in its nodes that begin to behave as free masses conserving their initial velocity. This erosion model represents a numerical remedial to great distortion that can cause excessive deformation of the mesh. After the blast is detonated, the deck parts begin to deform when shock fronts reach the deck. Due to the coupling effect between bridge and air, the deformation increases until the erosion limit is reached. The pressures destroy the deck just under the explosion allowing the blast wave to pass to the stiffened structures below. With the propagation of shock wave downwards, the deck is splitting like an irregular petal until the solution time is reached.

In order to analyze the dynamic responses generated in the deck of the bridge by a blast loading, four gauge points are defined in the model and are indicated in Fig. 10. These points are distributed in line with central axis on the deck. It can be seen that gauge point 1 is nearest to the explosive, while gauge point 4 the farthest. The distance between gauges 1 and 2 is 475 mm, gauges 2 and 3 1062 mm, gauges 3 and 4 938 mm. The principal variables of the analysis are saved at these gauge points.

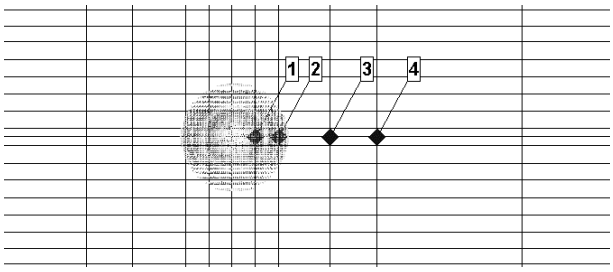

Fig.10 Gauge setting

The vertical velocity curves of these gauge points are presented in Fig. 11. It can be observed that these velocity values all tend to increase rapidly in the initial time, then gradually become stable, corresponding to the propagation law of blast wave in structures. Among these gauges, gauge 1, nearest to the explosion, is strongest affected with the greatest increment of velocity. Afterwards, its velocity value doesn't increase anymore, indicating the point has been destroyed and removed with that velocity. It is clear that the maximum velocities of the remaining three gauges are far lower than that of gauge 1. Furthermore, the farther the distance between gauge point and detonation point is, the lower the velocity gets tending to stabilize earlier which illustrates the least impact of blast wave.

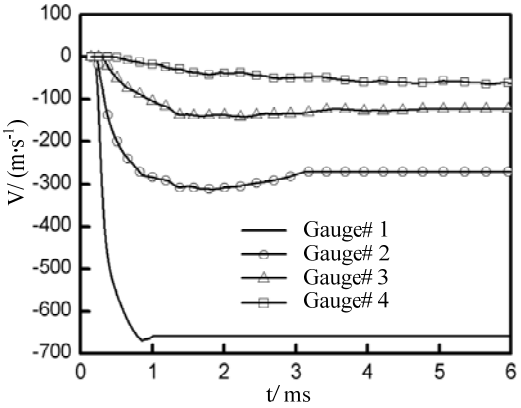

Fig.11 Velocity curves of gauges

The vertical acceleration curves of these gauge points are presented in Fig. 12. It can be seen that the acceleration response of gauge 1 is the greatest with the highest peak value. Accelerations of gauges 1 to 3 reach the peak values immediately after the blast detonation with small oscillations until the value is decreased to zero. This fact is due to the relatively high impact on structures in short duration of blast wave. Point 4 gets the least dynamic response due to the farthest distance from the explosion. It is noted that the acceleration responses of bridge can be used as an important input in damage detection and health monitoring of bridge structures under blast loads for further analysis.

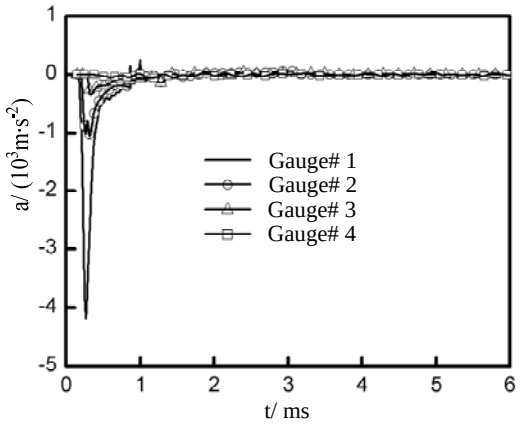

Fig.12 Acceleration curves of gauges

5. Conclusions

The numerical simulation and analysis of the structural damage of a steel truss bridge subjected to a blast load is presented in this paper. All the process from the detonation of the explosive charge to the broken deck, including the propagation of the blast wave and its interaction with the structure is reproduced.

The good agreement of peak overpressures between empirical expressions and numerically obtained values using a 5 cm mesh guarantees the effectiveness of blast loading and reliability of computational results.

The numerical analysis reproduces the destruction zone in bridge. The deck just under the explosion is damaged and cracked like an irregular petal while others keep almost intact. It illustrates that the characteristic of damage effect of a blast load to the whole bridge is limited destruction zone near the blast, which corresponds to the general law of explosion.

The numerical results provide a global understanding of bridge under blast loads. It may be generated to supplement experimental studies for developing appropriate blast-resistant design guidelines for bridges in the future.

Acknowledgements

This research is supported financially by the National Natural Science Foundation of China (No.50705058 and No. 50875166), the Ph.D. Programs Foundation of Ministry of Education of China (No.20070248113) and the National High Technology Research and Development Program of China (863 Program) （No.2007AA11Z234）.

References

[1] Williamson, E.B. and Marchand, K A. Recommendations for Blast-Resistant Design and Retrofit of Typical Highway Bridges, In: Structures Congress 2006: *Structural Engineering and Public Safety*, 2006, pp:1-6.

[2] Anwarul Islam, A.K.M. and Yazdani, N. Blast capacity and protection of AASHTO girder bridges, In:Proceedings of the Congress 217， *Forensic Engineering*, 2006, pp.311－326

[3] Federal Highway Administration (FHWA) Recommendations for bridge and tunnel security. Blue Ribbon Panel on Bridge and Tunnel Security, January 25, 2003.

[4] Winget, D.G., Marchand, K. A. and Williamson, E.B. Analysis and design of critical bridges subjected to blast loads, *ASCE Journal of Structural Engineering*, Vol.131, No. 8, 2005, pp.1243-1255.

[5] Baker, W.E., Cox, P.A., Westine, P.S., Kulesz, J.J. and Strehlow, R.A. *Explosion hazards and evaluation*. Amsterdam: Elsevier, 1983.

[6] Kinney, G.F. and Graham, K.J *Explosive shocks in air*, 2nd ed. Berlin: Springer Verlag, 1985.

[7] Smith, P. D. and Hetherington, J. G. *Blast and ballistic loading of structures*. London: Butterworth-Heinemann Ltd, 1994.

[8].Mair, H.U., Benchmarks for Submerged Structure Response to Underwater Explosions, Shock and Vibration, Vol.6, No. 4, 1999, pp. 169–181.

[9] ANSYS AUTODYN User Manual v11.0 (2007). Century Dynamics Inc.

[10] Robertson, N. J., Hayhurst, C. J., Fairlie, G. E. Numerical simulation of explosion phenomena. *International Journal of Computer Applications in Technology*. Vol.7, No. 3-6, 1994, pp. 316–329.

[11] Robertson, N., Hayhurst, C., Fairlie, G. Numerical simulation of impact and fast transient phenomena using AUTODYN-2D and 3D. *Nuclear Engineering and Design*. Vol.150, No. 2-3, 1994, pp. 235-241.

[12] Hayhurst, C. J., John Ranson, H., Gardner, D. J. Modelling of microparticle hypervelocity oblique impacts on thick targets. *International Journal of Impact Engineering*. Vol.17, No. 1-3, 1995, pp. 375-386.

[13] Formby, S.A. and Wharton, R.K. Blast characteristics and TNT equivalence values for some commercial explosives detonated at ground level, *Journal of Hazardous Materials*, Vol.50, No. 2-3, 1996, pp. 183–198.

[14] Baker, W.E., *Explosions in Air*, University of Texas Press. Austin, TX, 1973.

[15] Oran, E.S. and Boris, J.P. *Numerical simulation of reactive flow*. Elsevier,1987.

[16] Liu, S.H., Wei, J.D. and Qian Y.J. State-of-the art of research and analysis of structure and bridge under blast loads, *Journal of Shanghai Jiaotong University*, Vol.24, No. 3, 2005, pp. 16-19.